Astron. Astrophys. 312, 357–364 (1996)

ASTRONOMY AND ASTROPHYSICS

Excitation and temperature of extended gas in active galaxies

I. Observations*

Thaisa Storchi-Bergmann[1], Andrew S. Wilson[2,3], John Scott Mulchaey[4], and Luc Binette[5,3]

[1] Departamento de Astronomia, IF-UFRGS, CP 15051, CEP 91501-970, Porto Alegre, RS, Brasil
[2] Astronomy Department, University of Maryland, College Park, MD 20742, USA
[3] Space Telescope Science Institute, 3700 San Martin Drive, MD 21218, USA
[4] Observatories of the CIW, 813 Santa Barbara St., Pasadena, CA 91101, USA
[5] Observatoire de Lyon, UMR CNRS 5574, 9 Avenue Charles André, F-69561 St-Genis-Laval Cedex, France

Received 6 November 1995 / Accepted 21 December 1995

Abstract. We have obtained long-slit spectroscopy of five active galaxies showing extended high excitation emission lines reaching distances of several kiloparsecs from the nuclei. Measurement of the fluxes of weak lines, such as [OIII]λ4363 and HeIIλ4686, requires careful subtraction of the contribution of the stellar population, and the procedure for this subtraction is discussed in detail. For each galaxy, we present emission-line ratios for the nucleus and the extended gas at the most distant locations for which the fluxes of the weaker high excitation lines can be measured with an uncertainty $\leq$30%. In a companion paper (Paper II), these line ratios are used in a reevaluation of photoionization models of extended gas in active galaxies.

Key words: galaxies: active – galaxies: ISM – galaxies: nuclei – galaxies: Seyfert

1. Introduction

High excitation narrow emission-lines (from the narrow line region, NLR) are a characteristic property of many types of active galactic nuclei. Most studies (e.g. Koski 1978) have concentrated on the properties of the unresolved nucleus. However, many galaxies show spatially extended line emission that may reach several kpc from the nuclei in Seyfert galaxies (the extended narrow line region, ENLR) and up to a hundred kpc or more from the nuclei of radio galaxies (the extended emission line region, EELR). There are two advantages to studying the extended gas. First, the distance of the gas cloud from the nuclear source can be measured directly. Second, at distances in excess of a few kpc from the nucleus, the gas is generally in the low density limit for all commonly observed forbidden emission lines, which greatly simplifies modelling.

Models in which individual optically thick clouds are photoionized by an ultraviolet and soft x-ray continuum are quite successful in reproducing many of the emission-line ratios (e.g. Ferland & Osterbrock 1986; Robinson et al. 1987). However, as discussed more fully in the companion paper (Binette, Wilson & Storchi-Bergmann 1996, hereafter Paper II), there are three outstanding problems in modelling both the nuclear and extended gas, namely the models predict too weak high excitation lines, too small a range in the HeIIλ4686/Hβ ratio and too low electron temperatures. The last problem was highlighted by Tadhunter, Robinson & Morganti (1989, TRM89), who showed that the observed [OIII]λ4363/λ5007 ratio in twelve EELR's implies electron temperatures in the range 12,800K $<$ Te $<$ 22,000K, whereas the otherwise successful photoionization models predict Te $<$ 11,000K. TRM89 discussed several possibilities which might account for this discrepancy, including additional heating sources (plausibly cosmic rays or shocks) or metal abundances lower than the solar values assumed in the models.

As low electron temperatures are a cornerstone of the belief that the gas is ionized by photons, we considered it important to follow up and attempt to check the results of TRM89. This project is also timely in an instrumental sense, in that CCD's with good quantum efficiency in the blue are now available and allow considerably higher sensitivity spectra to be obtained in the vicinity of the weak [OIII]λ4363 line than was possible with systems based on image intensifiers (e.g. the Image Photon Counting System). We have, therefore, obtained long slit spectra of five active galaxies known from previous work to contain high excitation, extended nebulosities with the goal of accurately measuring the strength of [OIII]λ4363 and other diagnostic weak emission lines. In this paper, we present the results of the observations, giving emission-line ratios for both the nuclei and nebulosities at considerable distances ($>$ 2 kpc) from

* Based upon data obtained at the Cerro Tololo Interamerican Observatory, operated by the Association of Universities for Research in Astronomy, Inc. under contract with the National Science Foundation.

Table 1. Basic data[1]

Galaxy	Type	Activity	cz (km s^{-1})	Scale[2] (pc/arcsec)
NGC 526A	S0 pec?	Sy 1.9	5762±100	360
Mrk 573	(R)SAB(rs)0+:	Sy 2	5096±30	320
PKS 0349-278	E	Radio galaxy	19846±130	1143
ESO 362-G8	S0?	Sy 2	4785±24	301
PKS 0634-206	E	Radio galaxy	16548±30[3]	971
NGC 1097[4]	SB(rs)bc	LINER	1271±15	82
NGC 1386[5]	Sa	Sy 2	890±20	82

[1]From NASA/IPAC Extragalactic Database
[2]H_0=75 km s^{-1}Mpc^{-1} and q_0 = 0.5
[3]This work
[4]Storchi-Bergmann, Wilson & Baldwin 1996
[5]Weaver, Wilson & Baldwin 1991

Table 2. Log of observations

Galaxy	Date obs.	p.a. (°)	parall. (°)[1]	air mass[2]	exp. time (sec)
NGC 526A	5/6 Dec. 94	124	0	1.005	3600
Mrk 573	6/7 Dec. 94	125	131	1.637	1800
PKS 0349-278	5/6 Dec. 94	82	102	1.060	3600
ESO 362-G8	5/6 Dec. 94	60	78	1.068	3600
PKS 0634-206	5/6 Dec. 94	139	129	1.120	3600
NGC 1097	5/6 Dec. 94	90	0	1.002	1200
NGC 1386	5/6 Dec. 94	1	0	1.010	1800

[1]Parallactic angle in the middle of the integration
[2]In the middle of the integration

the nuclei. The companion paper (Paper II) describes extensive photoionization modelling and comparison with the line ratios and develops a new interpretation of the excitation sequence in active galaxies.

In Sect. 2, we describe the individual objects studied, while Sect. 3 is devoted to a description of the observations and reductions. Sect. 4 discusses the removal of stellar absorption features from the spectra, and results are given in Sect. 5. Our conclusions are presented in Sect. 6.

2. Objects observed

We have obtained spectra of the nucleus and regions of extended ionized gas in five active galaxies, three of which are Seyfert galaxies and two radio galaxies.

NGC 526A is an S0 galaxy with an emission-line spectrum showing a broad component in Hα but not in Hβ, and so can be classified as a Seyfert 1.9 (Osterbrock 1989). It belongs to a group of at least 5 members (Kollatschny & Fricke 1989) including a close companion, NGC 526B, located only 40″ (14.4 kpc, for H_0=75 km s^{-1}Mpc^{-1}, and q_0 = 0.5, used throughout this paper) to the SE. The galaxy is detected in X-rays (Griffiths et al. 1979) and radio emission (Unger et al. 1987). An image from the ESO plates as well as spectroscopy of the nucleus can be found in Fricke & Kollatschny (1989). Emission-line images recently obtained by Mulchaey, Wilson & Tsvetanov (1996) reveal a high excitation, bi-polar nebulosity of total extent ∼ 20″(7.2 kpc).

Mrk 573 is an S0 galaxy with a Seyfert 2 spectrum. It has a triple radio source – central component and two lobes displaced by 1.5″ (0.5 kpc) along the radio axis p. a. 125°. Narrow-band images and long-slit spectroscopy are given by Tsvetanov & Walsh (1992), who show that the high excitation gas extends ∼15″ (4.8 kpc) along the radio axis. Pogge & De Robertis (1993) present narrow-band images in [OIII]λ5007 and Hα+[NII]λλ6548,84 which show that the elongated structure observed by Tsvetanov & Walsh has a bi-conical shape.

PKS 0349-278 is a double lobe radio source with an extension of ∼450 kpc at p.a.∼55°(Baum et al. 1988), being the largest elliptical galaxy in a region of relatively high local density (4 galaxies within 80 kpc projected distance). [OIII]λ5007 images (Hansen, Nϕrgaard-Nielsen & Jϕrgensen 1987; Baum et al. 1988) show emission extending by ∼30″ (34 kpc) along p.a.∼90°, coincident with the direction of a close companion at ∼20″(23 kpc) E. Long-slit spectroscopy has been obtained by Danziger et al (1984), and reveals a complex velocity field with a total amplitude of ∼800 km s^{-1}. These authors interpret their observations in terms of a disc or concentric rings of gas with both rotational and radial motions.

ESO 362-G8 is an S0 galaxy with a Seyfert 2 spectrum, imaged by Mulchaey et al. (1996). The [OIII]λ5007 and Hα+[NII] images show emission extending ∼30″(9.0 kpc) along the highly inclined disk of the galaxy in p.a.∼165°, as well as a detached high excitation blob at ∼10″ (3.0 kpc) from the nucleus along p.a. 60°.

PKS 0634-206 is another radio galaxy with a double-lobed radio structure (Baum et al. 1988) extending ∼ 870 kpc along p.a.∼0°. An [OIII]λ5007 image in Hansen, Nϕrgaard-Nielsen & Jϕrgensen (1987) shows a Z-shaped structure extending ∼40″(39 kpc), with the central "arm" of the Z along p.a.∼140°. The innermost emission forms an elongated structure with the long axis in p.a.∼50°. Fosbury et al. (1984) have published long slit spectra along p.a. 178°, close to the radio source axis.

Basic data for the above galaxies – morphological types, nature of the activity, redshifts and scales (pc arcsec^{-1}) – are collected in Table 1.

3. Observations and data reduction

High signal-to-noise ratio (S/N) long-slit spectra of the sample galaxies were obtained using the 4m telescope, Cassegrain Spectrograph and a Reticon CCD detector at the Cerro Tololo Inter-American Observatory, on the nights of Dec. 5 and 6 of 1994. The seeing was ∼1″, the spectral resolution ∼8Å and the spectral range of the observations 3300-7450Å. There is some second order contamination for wavelengths larger than 6600Å, but the effect is only noticeable in the continuum, and does not affect the emission lines. The slit width was 220μm, corresponding to 1.5″ in the sky, and the scale of the frames in the spatial direction is 0.93″pixel^{-1}. The orientation of the slit was selected according to the morphology of the galaxy in narrow-band emission-line images, in order to sample the brightest and farthest high excitation gas. In order to minimize

Table 3. Observed emission-line ratios[1]

Line ident.	(1)	(2)	(3)	(4)	(5)	(6)[2]	(7)	(8)	(9)	(10)
[NeV]3346	0.9				2.5				5.6	8.0
[NeV]3426	5.1	2.1	4.4	3.9	5.0	11.9	3.4	3.7	14.6	23.4
[OII]3727	18.6	72.7	110.1	45.6	37.3	11.6	25.3	12.4	5.8	2.9
H10					0.9					2.5:
[NeIII]3869	8.4	12.3	13.0	10.8	9.6	9.4:	10.6	5.6	6.9	6.2
H8+HeI	1.3	3.8	2.7	1.1	1.2		1.7	1.3	1.0	
[NeIII]+Hε	3.6	6.8	7.0	4.7	4.1		4.6	1.6	3.0	2.7
[SII]4069+4076	0.7	1.8	1.6				0.8			
Hδ	1.6	4.2	4.7	2.2	2.0		2.5	1.0	2.3	1.3:
Hγ	2.7	7.6	9.4	4.5	4.1		3.8	2.5	2.7	3.2
[OIII]4363	1.6	2.3	1.6::[3]	1.8	1.6		1.1	0.5::[3]	1.8	1.7:
He I 4471		0.9								
HeII 4686	2.3	2.4	2.3	3.5	3.2		3.5	2.8	4.3	6.6
Hβ	6.4	14.6	20.1	9.2	9.5	2.1:	9.2	7.9	8.4	9.6
[OIII]4959	33.	32.5	32.1	33.8	32.9	32.8	32.0	32.7	34.3	32.2
[OIII]5007	Sat	100.	100.	100.	100.	100.	100.	100.	100.	100.
[NI]5200		1.0	2.7							
HeI 5876	0.8	2.2					1.3			
[FeVII]6086								2.9		
[OI]6300	3.6	6.8	18.0	1.3	1.7		1.7	4.6		
[OI]6364	1.5	2.5	7.0				0.7:	1.3		
[NII]6548	8.7	15.4	19.4			15.5	8.1	10.6		
Hα narrow	35.4	45.9	57.7	27.4	25.4	33.2	32.8	56.8	29.5	37.0
Hα broad	107.8									
[NII]6584	24.2	46.2	45.1	13.1	8.5	58.9	24. 9	29.3	5.8	4.6
[SII]6716	7.8	23.3	36.4	8.4:	6.0:	9.4	7.6	12.3	1.7	2.5:
[SII]6731	9.6	16.2	22.2	3.0:	3.5:	8.5	5.3	10.2	1.3	1.5:
[AIII]7136		2.7					3.4	5.5		

[1]Fluxes relative to [OIII]λ5007=100. When this line was saturated, they are relative to [OIII]λ4959=33. Identification of the spectra: (1) NGC 526A – nucleus; (2) NGC 526A – 7″NW of nucleus; (3) PKS 0349-278 – nucleus; (4) PKS 0349-278 – 11″NE of nucleus; (5) PKS 0349-278 – 11″SW of nucleus; (6) ESO362-G8 – nucleus; (7) ESO362-G8 – 10″NE of nucleus; (8) PKS 0634-206 – nucleus; (9) PKS 0634-206 – 6″SE of nucleus; (10) PKS 0634-206 – 10″NW of nucleus

[2]Lines in nr. (6) uncertain due to strong A type stellar population.

[3]upper limit

effects of differential atmospheric refraction, the observations were scheduled so that the slit direction was always close to the parallactic angle. All galaxies were observed with air masses lower than 1.1, except Mrk 573, for which the air mass was 1.64; however, the parallactic angle differed by only ~6° from the position angle of the slit. A log of the observations is shown in Table 2, which gives the date of observation, slit p.a., parallactic angle, air mass and exposure time.

The spectra were reduced (including flux calibration) using standard procedures in IRAF. One-dimensional spectra were extracted by binning together 3 pixels for the nuclear and adjacent regions and 6 pixels for the fainter, outer regions. The spectra were then corrected for atmospheric absorption of H_2O and O_2 at near-infrared wavelengths, by dividing the spectra of the galaxies by the spectra of hot standard stars, after removing the absorption features in the stellar spectra and normalizing the slope of their continua to unity.

The extracted spectra were then inspected for the presence of the λ4363 emission line. For our study of emission-line ratios, we have selected the spectra of the nuclei and the most distant regions from the nuclei at which it was still possible to measure the flux of the λ4363 line with an uncertainty ≤30%. The locations of these regions are 7″NW of the nucleus for NGC 526A, 6″NW and SW for Mrk 573, 11″SW and NE for PKS 0349-278, 10″NE for ESO 362-G8 and 10″NW and 6″SE for PKS 0634-206.

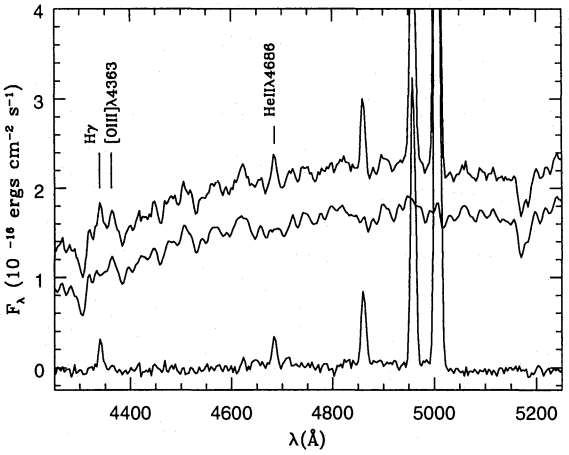

Fig. 1. Illustration of the procedure for subtraction of the stellar population in the spectral region including [OIII]λ4363 and HeIIλ4686, showing the necessity of an accurate subtraction of the stellar population for reliable measurements of these two emission lines. Top: nuclear spectrum of PKS 0634-206; middle: stellar population template T1097, with an arbitrary vertical shift for clarity; bottom: difference between nuclear and stellar population spectra. [OIII]λ4363 is not detected in the nucleus of PKS 0634-206.

4. Analysis - the stellar population

All the sample galaxies have prominent stellar absorption features and, in order to obtain accurate fluxes in the fainter lines (e.g. [OIII]λ4363), it is necessary to subtract the contribution of

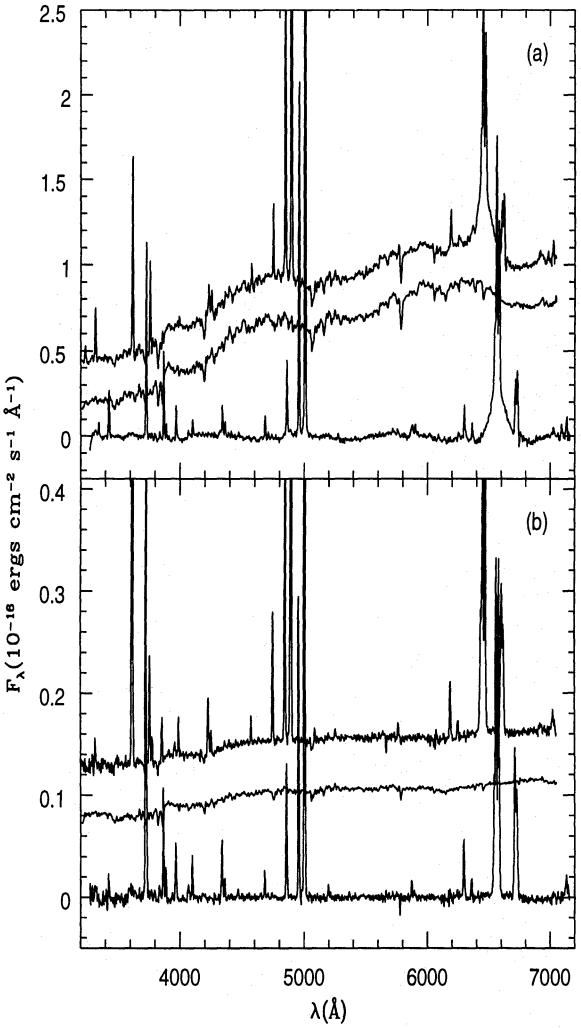

Fig. 2. a Top: nuclear spectrum of NGC 526A; middle: stellar population template T1097 normalized to the flux of the nuclear spectrum; bottom: the difference between the two. The top and middle spectra have been shifted horizontally and vertically for a better visualization of the difference spectrum, which is plotted in the rest frame of the galaxy as absolute flux *vs* wavelength. **b** Same as in **a** for the spectrum of extended gas at 7″NW from the nucleus.

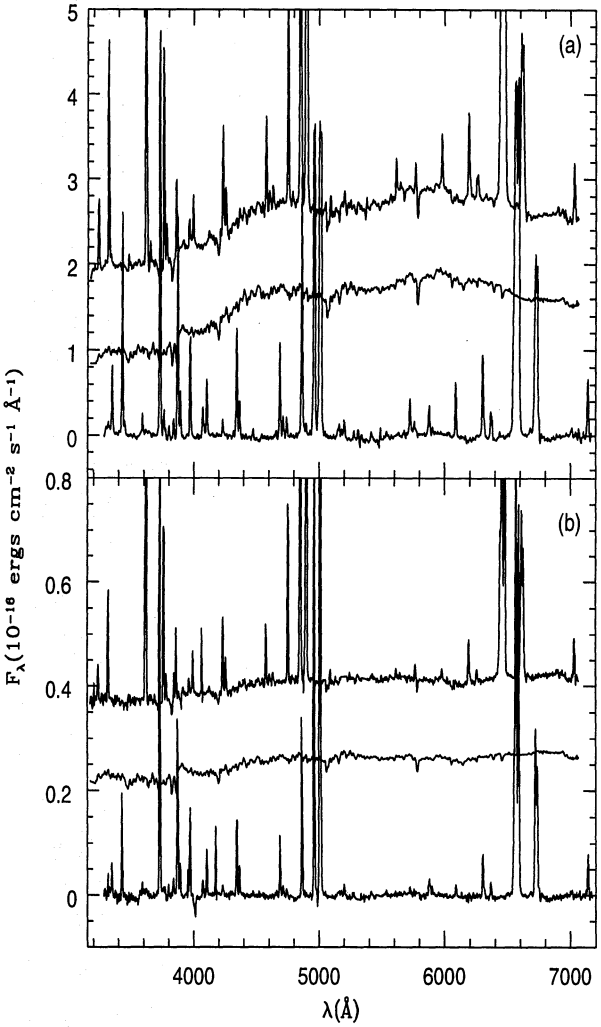

Fig. 3. a Same as fig. 2a for Mrk 573. **b** Same as fig. 2a for extended gas at 6″NW from the nucleus of Mrk 573.

the stellar population. We have, therefore, used long-slit spectra of two nearby galaxies, the spectra of which are less contaminated by emission lines than the sample galaxies, to construct stellar population templates. The spectrum of the bulge of NGC 1097 was used to represent the nuclear stellar population spectrum of most galaxies, and that of the disk of NGC 1386 was used to represent the stellar population of the disks of the galaxies. These galaxies were selected, among other archival data we have, on the basis of the quality of the match of their spectra to the stellar population features in the sample galaxies and the high signal-to-noise ratio of the spectra.

The first template was obtained from the average of two spectra of the bulge of NGC 1097 (hereafter identified as T1097), extracted from windows of size 1.5″×2.8″ centered at ∼4″ E and W of the nucleus. The resulting average spectrum was edited to eliminate the emission lines still present in the spectra, using template spectra from the library of Bica (1988), which are free of emission lines, to interpolate the spectra in the edited regions. This procedure is preferable to the direct use of Bica's templates, because of their lower spectral resolution (∼20Å) than our observations.

The second template was constructed by averaging two spectra of the disk of NGC 1386 (hereafter identified as T1386), from windows of size 1.5″×2.8″ centered at 8.4″ S and N of the nucleus. The emission lines were eliminated using the same method as described above for NGC 1097.

The templates were then redshifted to the radial velocities of the sample galaxies, normalized to the same flux level as the galaxies at ∼ λ5870 and compared with them. Some mismatch between the continua of the galaxies and the templates were found redward of 6600Å, presumably due to second order contamination. A low order spline was then used to adjust the

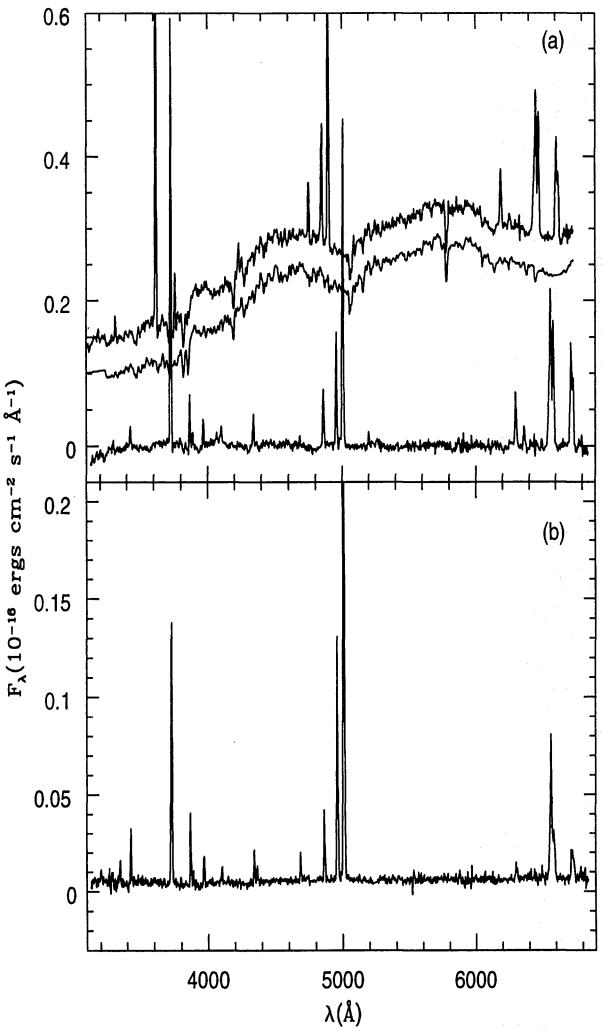

Fig. 4. a Same as fig. 2a for PKS 0349-278. **b** Spectrum of extended gas at 11″SW from the nucleus, where the stellar population contribution is negligible.

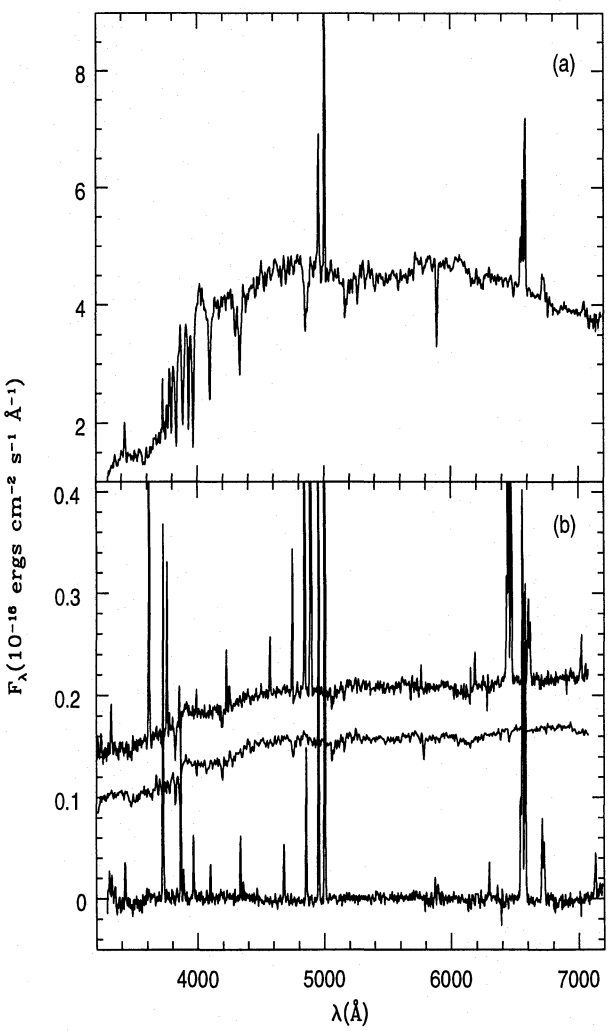

Fig. 5. a Nuclear spectrum of ESO 362-G8. **b** Top: Spectrum of extended gas at 10″NE from the nucleus; middle: stellar population template T1386 normalized to the flux of the top spectrum; bottom: the difference between the two. The top and middle spectra have been shifted horizontally and vertically for a better visualization of the difference spectrum, which is plotted in the rest frame of the galaxy as absolute flux *vs* wavelength.

overall shape of the continuum of the template to that of each galaxy.

A careful subtraction of the stellar population template is particularly important for measurements of faint lines, such as [OIII]λ4363 and sometimes HeIIλ4686, as illustrated in Fig. 1. It can be seen that there is a feature in the stellar template T1097 which is very close to the wavelength of the [OIII]λ4363 line. An apparent "emission" feature of equivalent width ∼1Å is also seen in the spectrum of the nucleus of PKS 0634-206, but this feature practically disappears after the template is subtracted. This feature in the stellar population is also present in template T1386 with similar equivalent width. Figure 1 shows that the HeIIλ4686 line can also be confused with a feature in the stellar spectrum, but in this case, the line only *appears* convincingly after the population subtraction.

It was concluded that the template T1097 is a good representation of the stellar population in the nuclei of all sample galaxies except ESO 362-G8. This template was also used for the regions 6″NW and SE of the nucleus in Mrk 573. T1386 is a good representation of the stellar population at 7″NW of the nucleus in NGC 526A and at 10″NE of the nucleus of ESO 362-G8. It was not possible to find a suitable template for the nuclear spectrum of ESO 362-G8, which shows strong Balmer absorption lines typical of the spectra of A stars. In the cases of the extranuclear spectra of PKS 0349-278 and PKS 0634-206, the contribution of the continuum is negligible, so it was not necessary to subtract a stellar template. Figures 2-6 show the nuclear spectrum and one spectrum of the extended gas for each galaxy, together with the adopted stellar population template and the difference between the galaxy spectra and the stellar template.

Table 4. Observed emission-line ratios for Mrk 573[1]

Line ident.	nucleus	6″NW	6″SE
[NeV]3346	2.0	1.6	2.2
[NeV]3426	6.5	5.2	7.2
OIII 3444	0.4		
He I 3587	0.5		
[OII]3727	14.4	27.7	20.3
[FeVII]3760+(OIII)	0.7		
H10	0.5	0.8	
H9	0.7	0.8	
[NeIII]3869	7.1	10.5	10.3
H8+HeI	1.6	1.8	1.9
[NeIII]+Hϵ	3.5	4.9	4.0
[SII]4069(+4076)	1.2	1.2	0.7
Hδ	1.9	2.5	2.2
[FeV]4228	0.5	0.7	
Hγ	3.6	4.3	3.5
[OIII]4363	1.2	1.3	1.4
HeI 4471	0.4		0.5
HeII 4686	3.2	3.1	2.8
[AIV]4711	0.8	0.8	0.7
[AIV]4740	0.6	0.5	0.7
Hβ	8.0	9.0	7.8
[OIII]4959	31.7	34.9	32.1
[OIII]5007	100.	100.	100.
[NI]5200	0.6	0.6	0.8
[FeVII]5721	1.2		
[NII]5755	0.2		
HeI 5876	1.2	1.3	0.8
[FeVII]6086	1.9	0.7	0.8
[OI]6300	3.0	2.4	2.2
[SII]6312	0.3	0.7	0.4
[OI]6364	0.9	1.0	0.7
[FeX]6374	0.6		
[NII]6548	8.4	10.5	11.1
Hα	30.4	36.9	49.3
[NII]6584	25.6	27.6	32.3
[SII]6716	8.2	11.9	14.2
[SII]6731	8.3	8.4	11.6
[AIII]7136	2.6	3.0	4.4
[OII]7319	0.8		
[OII]7330	0.6		

[1]Fluxes are relative to [OIII]λ5007=100. In the nuclear spectrum, [OIII]λλ4959,5007, Hα, [NII]λλ6548,6584 were all saturated. Their relative intensities were calculated, as described in the text, using line ratios given in Koski (1978).

Table 5. Reddening corrected emission-line ratios[1]

Line ident.	(1)	(2)	(7)	(8)	(9)	(10)
[NeV]3346	2.7				7.1	11.7
[NeV]3426	13.8	2.1	4.4	15.9	18.0	33.5
[OII]3727	38.8	74.0	30.4	36.8	6.8	3.7
H10						3.2:
[NeIII]3869	15.6	12.5	12.5	14.3	7.9	7.8
H8+HeI	2.4	3.8	1.9	3.2	1.2	
[NeIII]+Hϵ	6.2	6.9	5.3	3.7	3.4	3.3
[SII]4069,76	1.1	1.8	0.9			
Hδ	2.5	4.3	2.8	2.1	2.5	1.5:
Hγ	3.7	7.7	4.1	4.0	2.9	3.6
[OIII]4363	2.1	2.3	1.1	0.8::[2]	1.9	1.9:
He I 4471		0.9				
HeII 4686	2.7	2.4	3.6	3.5	4.4	6.9
Hβ	6.7	14.6	9.3	8.7	8.6	9.8
[OIII]4959	33.	32.5	32.2	33.8	34.6	32.4
[OIII]5007	Sat.	100.	100.	100.	100.	100.
[NI]5200		1.0				
HeI 5876	0.5	2.2	1.2			
[FeVII]6086				1.7		
[OI]6300	2.3	6.7	1.6	2.4		
[OI]6364	0.9	2.5	0.6:	0.7		
[NII]6548	5.1	15.2	7.1	5.1		
Hα narrow	20.7	45.4	28.9	27.0	26.6	30.5
Hα broad	63.0					
[NII]6584	14.1	45.7	21.9	13.8	5.2	3.8
[SII]6716	4.4	23.0	6.6	5.5	1.5	2.0:
[SII]6731	5.4	16.0	4.6	4.5	1.1	1.2:
[AIII]7136		2.6	2.9	2.2		
Av (mag)	1.8	0.04	0.4	2.5	0.4	0.6

[1]Fluxes relative to [OIII]λ5007=100. When this line was saturated, they are relative to [OIII]λ4959=33. Identification of the spectra: (1) NGC 526A – nucleus; (2) NGC 526A – 7″NW of nucleus; (7) ESO362-G8 – 10″NE of nucleus; (8) PKS 0634-206 – nucleus; (9) PKS 0634-206 – 6″SE of nucleus; (10) PKS 0634-206 – 10″NW of nucleus

[2]upper limit

5. Results

The emission lines were measured from the stellar population-subtracted spectra by fitting one Gaussian to each line, except in NGC 526A for which we used two Gausssian components to describe Hα, due to the presence of a clear broad component. The procedure adopted for deblending Hα(narrow)+[NII]λλ6548,84 and [SII]λλ6717,31 was to constrain the line widths in each blend to be identical. In Table 3, we present the fluxes of the observed emission lines relative to Hβ, for the nuclear and extranuclear spectra for all galaxies except Mrk 573, the fluxes of which are presented in Table 4. The reddening was calculated from the Balmer decrement $H\alpha/H\beta$ assuming an intrinsic value of 3.1. Tables 5 and 6 show the reddening corrected emission line fluxes, except for PKS 0349-278, which has no measurable reddening, and the nucleus of ESO 362-G8, for which it was not possible to measure Hβ. The measurement uncertainties for most emission lines are smaller than 10%. For the fainter lines, such as [SII]λ4069,4076, [OIII]λ4363, [NI]λ5200, and [OI]λ6363, the uncertainties are about 20%. A colon identifies emission lines with uncertainties ~30-40%. For the nuclear spectra of PKS 0349-278 and PKS 0634-206, the listed [OIII]λ4363 fluxes are upper limits.

We now comment on the emission line spectra for each galaxy.

NGC 526A - This galaxy has a Seyfert 1.9 nucleus, as evidenced by the broad component in Hα and its absence in Hβ. [OIII]λ5007 emission can be traced up to 13″NW and all the way to the companion galaxy, NGC 526B, located at 40″SE of NGC 526A. From line ratios such as [OIII]λ4959/Hβ and HeIIλ4686/Hβ, it can be concluded that the gaseous excitation is higher in the nucleus than in the extended gas at 7″NW. The line ratio [SII]λ6717/λ6731 indicates higher density at the nucleus than in the extended gas. The absorption feature NaIλ5890 was slightly oversubtracted in the nuclear spectrum, introducing an spurious emission feature longward of HeIλ5876.

Mrk 573 - In the nuclear spectrum of this Seyfert 2 galaxy, the lines [OIII]λλ4959,5007, Hα, and [NII]λλ6548,84 are all saturated. Their relative intensities were calculated using the line ratios given in Koski (1978), as follows. The [OIII] line intensities were obtained by multiplying our Hβ flux by the [OIII]/Hβ ratios given by Koski. Similarly, the Hα and [NII] intensities were obtained by multiplying our [SII]λλ6717,6731 flux by the Hα/[SII], [NII]/[SII] ratios given by Koski. Note that Koski's observations were made through a 2.7″×4.0″ aperture, which is larger than ours (1.5″×2.8″), so there could be systematic errors introduced by this procedure. Extended emission is observed up to at least 12″NW and 12″SE of the nucleus.

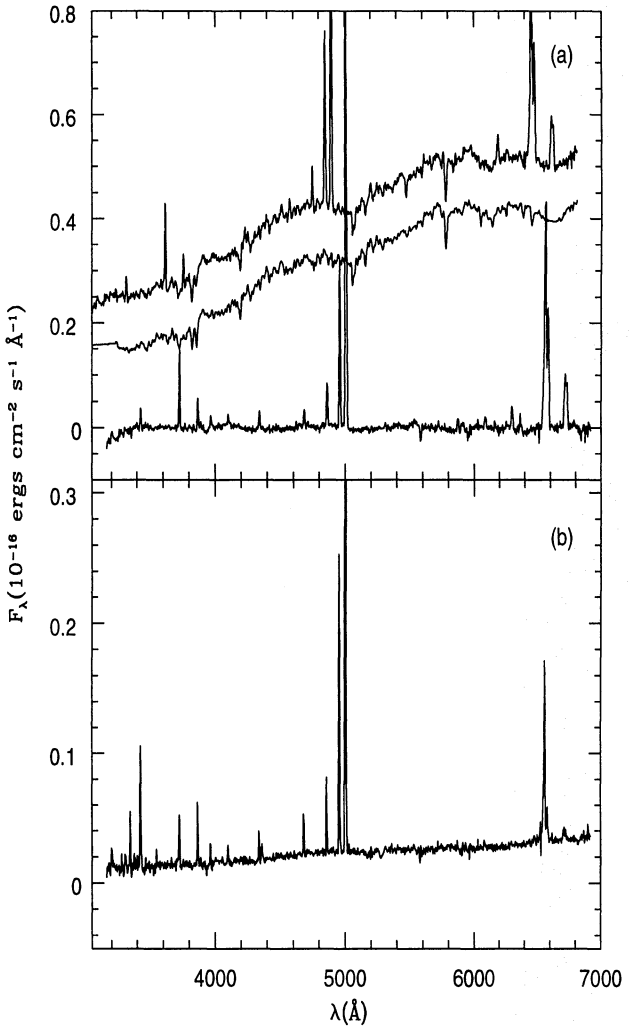

Fig. 6. a Same as fig. 2a for PKS 0634-206. **b** Spectrum of extended gas at 6″SE from the nucleus. Stellar population contribution is negligible.

Table 6. Reddening corrected emission-line ratios for Mrk 573[1]

Line ident.	nucleus	6″NW	6″SE
[NeV]3346	3.0	2.7	8.2
[NeV]3426	9.2	8.3	24.8
OIII 3444	0.6		
He I 3587	0.7		
[OII]3727	18.7	39.3	51.0
[FeVII]3760+	1.0		
H10	0.6	1.1	
H9	0.9	1.1	
[NeIII]3869	8.9	14.2	22.8
H8+HeI	2.0	2.4	4.1
[NeIII]+Hε	4.3	6.4	8.1
[SII]4069,76	1.4	1.5	1.3
Hδ	2.2	3.2	4.0
[FeV]4228	0.5	0.9	
Hγ	4.1	5.0	5.3
[OIII]4363	1.3	1.5	2.0
HeI 4471	0.4		0.6
HeII 4686	3.4	3.4	3.4
[AIV]4711	0.9	0.8	0.8
[AIV]4740	0.6	0.6	0.8
Hβ	8.1	9.3	8.4
[OIII]4959	32.0	35.2	32.8
[OIII]5007	100.	100.	100.
[NI]5200	0.6	0.6	0.7
[FeVII]5721	1.1		
[NII]5755	0.2		
HeI 5876	1.0	1.1	0.5
[FeVII]6086	1.6	0.6	0.5
[OI]6300	2.6	2.0	1.3
[SII]6312	0.3	0.5	0.2
[OI]6364	0.8	0.8	0.4
[FeX]6374	0.5		
[NII]6548	7.0	8.2	5.9
Hα	25.4	28.9	26.0
[NII]6584	21.3	21.6	16.9
[SII]6716	6.8	9.2	7.1
[SII]6731	6.8	6.5	5.8
[AIII]7136	2.1	2.2	2.0
[OII]7319	0.6		
[OII]7330	0.5		
Av (mag)	0.6	0.8	2.2

[1]Fluxes are relative to [OIII]λ5007=100. In the nuclear spectrum, [OIII]λλ4959,5007, Hα, [NII]λλ6548,6584 were all saturated. Their relative intensities were calculated, as described in the text, using line ratios given in Koski (1978).

The [SII]λλ6716/ 6731 ratio indicates that the nuclear gas has a higher density than the extranuclear regions. However, the nuclear and extranuclear regions have similar excitation.

PKS 0349-278 - This radio galaxy has a Seyfert 2 nuclear spectrum, and two blobs of strong high excitation emission at ∼ 11″NE and SW of the nucleus. Faint [OIII]λ5007 emission can be observed up to 57″NE and 36″SW. Emission from the companion galaxy is seen ∼20″E of the nucleus. The emission at 11″NE is blueshifted by 130 km s^{-1} and that at 11″SW is redshifted by 110 km s^{-1} relative to the nucleus, in agreement with the velocity curves presented by Danziger et al. (1984). The extended gas exhibits higher excitation than the nuclear gas. Our measurements of the off-nuclear [OIII]λ4363/5007 ratio agree well with those given by TRM89 for their "W" and "E" locations, although they do not specify exactly where these positions are.

ESO 362-G8 - Along p.a. 60°, emission in this Seyfert 2 galaxy is seen ∼ 6″ to both SW and NE. At 10″NE there is a detached blob with a high excitation spectrum. All emission lines at the nucleus have a small equivalent width due to the very strong continuum of a stellar population rich in A stars.

PKS 0634-206 - This radio galaxy has very similar characteristics to those of PKS 0349-278, namely a Seyfert 2 nuclear spectrum and two bright clouds at 6″SE and 10″NW with higher excitation (in terms of HeIIλ4686/Hβ and [NeV]λ3426/Hβ) than the nucleus. There is also a large velocity difference between the two clouds: the SE cloud is blueshifted by 255 km s^{-1} and the NW cloud is redshifted by 187 km s^{-1} relative to the nucleus of the galaxy. Beyond the NW cloud there is another fainter cloud of emission at 25″ NW.

6. Summary and conclusions

The main results from this paper can be summarized as follows.

Long-slit spectra of three Seyferts and two radio galaxies have revealed the presence of high excitation emission – including [NeV]λ3426, [OIII]λ4363 and HeIIλ4686 emission lines – at distances from the nuclei as large as 2-3 kpc for the Seyferts NGC 526A, Mrk 573 and ESO 362-G8, and 10 and 13 kpc for

the radio galaxies PKS 0634-206 and PKS 0349-278, respectively.

In NGC 526A, which has a Seyfert 1.9 nuclear spectrum, the excitation is larger at the nucleus than in the extended gas, perhaps because – considering the unified model for Seyfert's – we are observing gas closer in to the active nucleus than in the case of the galaxies with Seyfert 2 spectra. In Mrk 573 the excitation at the nucleus is similar to that 6″away, and for the radio galaxies PKS 0349-278 and PKS 0634-206 the excitation of the extended gas is higher than that of the nucleus.

We have shown that it is frequently necessary to subtract carefully the contribution of the underlying stellar population in order to measure reliably the fluxes of the emission lines [OIII]λ4363 and HeIIλ4686. In both the stellar population templates we used, there is a peak at a wavelength near 4363Å. This feature mimics an emission line with "equivalent width" near 1Å, and can lead to misleading results for the strength of [OIII]λ4363 if not carefully removed.

In the companion paper (Binette et al. 1996, Paper II), we use these results to reevaluate photoionization models of extended gas in active galaxies.

Acknowledgements. This research has made use of the NASA/IPAC Extragalactic Database (NED), which is operated by the Jet Propulsion Laboratory, Caltech, under contract with the National Aeronautics and Space Administration. TSB thanks the Brazilian institution CNPq for support for this research. This research was supported in part by NASA through grant NAGW-3268.

References

Baum, S. A., Heckman, T., Bridle, A., van Breugel, W. & Miley, G. 1988, ApJs, 68, 643
Bica, E. 1988, A&A, 195, 76
Binette, L. Wilson, A. S. & Storchi-Bergmann, T. 1996, A&A, submitted (Paper II)
Danziger, I. J., Fosbury, R. A. E., Goss, W. M., Bland, J., Boksenberg, A. 1984, MNRAS, 208, 589
Ferland, G. J. & Osterbrock, D. E. 1986, ApJ, 300, 658
Fosbury, R. A. E., Tadhunter, C. N., Bland, J. & Danziger, I. J. 1984, MNRAS, 208, 955
Fricke, K. J. & Kollatschny, W. 1989, A&AS, 77, 75
Griffiths, R. E., Doxsey, R. E., Johnston, M. D., Schwartz, D. A., Schwarz, J. & Blades, J. C. 1979, ApJlett, 230, 21
Hansen, L., Nϕrgaard-Nielsen, H. U. & Jϕrgensen, H. E. 1987, A&AS, 71, 465
Kollatschny, W. & Fricke, K. J. 1989, A&A, 219, 34
Koski, A. 1978, ApJ, 223, 56
Mulchaey, J. S., Wilson, A. S. & Tsvetanov, Z. I. 1996, ApJS, in press
Osterbrock, D. E. 1989, Astrophysics of Gaseous Nebulae and Active Galactic Nuclei, University Science Books, Mill Valley, California
Pogge, R. W. & De Robertis, M. M. 1993, ApJ, 404, 563
Robinson, A., Binette, L., Fosbury, R. A. E., Tadhunter, C. N 1987, MNRAS, 227, 97
Storchi-Bergmann, T., Wilson, A. S. & Baldwin 1996, ApJ, in press
Tadhunter, C. N., Robinson, A., Morganti, R., 1989, in: ESO Workshop on Extranuclear Activity in Galaxies, Eds. Meurs, E. J. A., Fosbury, R. A. E., ESO Conf. and Workshop Proc. No. 32, Garching, p.292 (TRM89)
Tsvetanov, Z. & Walsh, J. R. 1992, ApJ, 386, 485
Ulvestad, J. S. & Wilson, A. S. 1984, ApJ, 285, 439
Unger, S. W., Lawrence, A., Wilson, A. S., Elvis, M., Wright, A. E. 1987, MNRAS, 228, 521
Weaver, K., Wilson, A. S. & Baldwin, J. A. 1991, ApJ, 366, 50

This article was processed by the author using Springer-Verlag LaTeX A&A style file version 3.